Gd-Based Single-Ion Magnets with Tunable Magnetic Anisotropy: Molecular Design of Spin Qubits

M. J. Martínez-Pérez,[1,2] S. Cardona-Serra,[3] C. Schlegel,[4] F. Moro,[5] P. J. Alonso,[1,2] H. Prima-García,[3] J. M. Clemente-Juan,[3] M. Evangelisti,[1,2] A. Gaita-Ariño,[3] J. Sesé,[6,2] J. van Slageren,[7] E. Coronado,[3,*] and F. Luis[1,2,†]

[1]*Instituto de Ciencia de Materiales de Aragón, CSIC-Universidad de Zaragoza, Pedro Cerbuna 12, 50009 Zaragoza, Spain*
[2]*Departamento de Física de la Materia Condensada, Universidad de Zaragoza, Pedro Cerbuna 12, 50009 Zaragoza, Spain*
[3]*Instituto de Ciencia Molecular (ICMol), Universidad de Valencia, Catedrático José Beltrán 2, 46980, Paterna, Spain*
[4]*1. Physikalisches Institut, Universität Stuttgart, Pfaffenwaldring 57, 70550 Stuttgart, Germany*
[5]*School of Chemistry, University of Nottingham, University Park, NG7 2RD Nottingham, United Kingdom*
[6]*Instituto de Nanociencia de Aragón, Universidad de Zaragoza, Edificio Investigación y Desarrollo, Campus Río Ebro, 50018 Zaragoza, Spain*
[7]*Institut für Physikalische Chemie, Universität Stuttgart, Pfaffenwaldring 55, 70569 Stuttgart, Germany*

(Received 22 February 2012; published 15 June 2012)

We report ac susceptibility and continuous wave and pulsed EPR experiments performed on GdW_{10} and GdW_{30} polyoxometalate clusters, in which a Gd^{3+} ion is coordinated to different polyoxometalate moieties. Despite the isotropic character of gadolinium as a free ion, these molecules show slow magnetic relaxation at very low temperatures, characteristic of single molecule magnets. For $T \lesssim 200$ mK, the spin-lattice relaxation becomes dominated by pure quantum tunneling events, with rates that agree quantitatively with those predicted by the Prokof'ev and Stamp model [Phys. Rev. Lett. **80**, 5794 (1998)]. The sign of the magnetic anisotropy, the energy level splittings, and the tunneling rates strongly depend on the molecular structure. We argue that GdW_{30} molecules are also promising spin qubits with a coherence figure of merit $Q_M \gtrsim 50$.

DOI: 10.1103/PhysRevLett.108.247213 PACS numbers: 75.50.Xx, 03.67.Lx, 75.30.Gw, 75.45.+j

Single molecule magnets (SMMs) [1] consist of a high-spin magnetic core encapsulated in a ligand shell. Crystals of SMMs represent a very attractive workbench for the investigation of quantum magnetism. They exhibit intriguing quantum phenomena, such as magnetization tunneling [2], Berry phase interference [3], quantum spin coherence [4–6], and quantum phase transitions [7]. In the last few years, SMMs have also emerged as candidates for the hardware of quantum computers [8–13].

Although most of the recent studies and proposals for applications are based on clusters with a polynuclear magnetic core, mononuclear SMMs (or single-ion magnets) are better suited to quantitatively test theories of quantum tunneling and coherence [14–16]. They also offer a better control over parameters that determine the energy level spectrum and wave functions as well as decoherence. For instance, inorganic polyoxometalate (POM) molecules can be prepared from elements with zero nuclear spin, thus giving access to nuclear-spin free systems [15]. In addition, the replacement of the magnetic ion by a nonmagnetic one (e.g. replacing a lanthanide with Y^{3+}) enables the synthesis of magnetically diluted crystals [17]. Well-known sources of decoherence [18] can therefore be reduced while preserving both the crystalline order and the molecular structure.

We here explore a new method for controlling the magnetic anisotropy of single lanthanide ions, which determines the splitting of the magnetic energy levels and the spin dynamics, via the chemical design of their first coordination sphere. We choose Gd^{3+} because, as a free ion, it has an isotropic electronic ground state with $L = 0$ and $S = 7/2$. It is therefore a model crystal-field probe: its magnetic anisotropy is almost exclusively determined by the Coulomb interaction with nearby ions [19]. In order to investigate this possibility, we compare potassium salts of two POM molecules, namely $[Gd(W_5O_{18})_2]^{9-}$ and $[Gd(P_5W_{30}O_{110})]^{12-}$ hereafter referred to as GdW_{10} and GdW_{30}, respectively (Fig. 1). Our results confirm that the magnetic anisotropy strongly depends on the molecular structure. These and other related molecules could therefore be designed and optimized with an eye on different applications of lanthanide spins, such as quantum computing [20].

Magnetic measurements in the region of 1.8 K $\leq T \leq$ 300 K were performed using a commercial SQUID magnetometer. The ac susceptibility measurements have been extended down to 13 mK using a microSQUID susceptometer installed inside the mixing chamber of a ^{3}He-^{4}He dilution refrigerator [21,22]. Heat capacity measurements from $T = 350$ mK up to room temperature were performed on a commercial physical measurement platform. Broadband electron paramagnetic resonance (EPR) spectroscopy was performed at $T = 1.7$ K and $T = 10$ K using a frequency tunable cavity [23]. Finally, pulsed EPR experiments on pure and magnetically diluted powder samples were performed using an Elexys X-band spectrometer.

The magnetization isotherms measured at and above $T = 2$ K (not shown) agree very well, for both clusters,

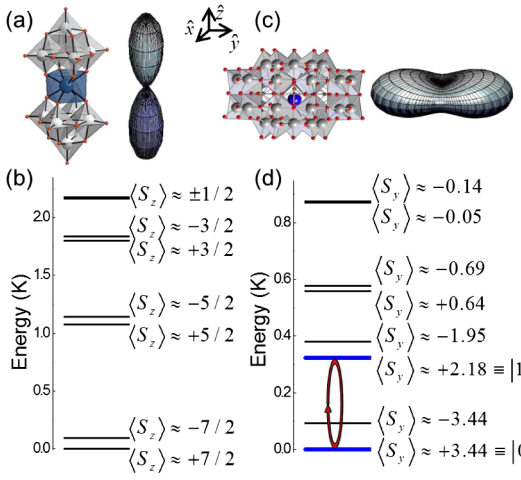

FIG. 1 (color online). (a) GdW_{10} molecule (left) and three-dimensional plot of the probability for its spin to point along any direction of space, calculated at $T = 0.5$ K (right). (b) Energy levels of GdW_{10} for $\mu_0 H_z = 10$ mT. (c) GdW_{30} molecule (left) and the corresponding probability plot at $T = 0.5$ K (right). (d) Energy levels of GdW_{30} for $\mu_0 H_y = 10$ mT.

with the behavior expected for isotropic $S = 7/2$ spins with a gyromagnetic ratio $g = 2$. Figure 2 shows ac susceptibility data (real component χ') measured on powdered GdW_{10} and GdW_{30} samples. These results show that their net spin is the same and that the magnetic anisotropy, if present, must be rather small. Differences between the two become apparent however if one compares their dynamical magnetic response at very low temperatures. Both $\chi'(T)$ sets of data show the dependence on frequency that is characteristic of the SMM behavior. But, while $\chi'(T)$ of GdW_{10} nearly vanishes below $T = 0.4$ K for a frequency $\omega/2\pi = 158$ Hz, the susceptibility blocking is not complete for GdW_{30}, i.e., no maximum is observed even at frequencies as high as $\omega/2\pi = 631$ kHz and temperatures in the close vicinity of absolute zero (13 mK).

The anisotropy parameters have been determined by fitting the experimental EPR spectra. Figure 3 shows two representative spectra, obtained at $T = 10$ K and a resonant frequency of 25 GHz, and the corresponding theoretical fits. The fits are performed with EasySpin [24] and are based on the following spin Hamiltonian:

$$\mathcal{H} = \sum_{n=\{2,4,6\}} B_n^0 \hat{O}_n^0 + \sum_{n=\{2,4,6\},0<m\leq n} B_n^m \hat{O}_n^m - g\mu_B(H_x S_x + H_y S_y + H_z S_z), \quad (1)$$

where the B_n^m's are crystal-field parameters and $\hat{O}_n^m$ are Stevens' equivalent spin operators [25]. These parameters depend on the Gd^{3+} local coordination. In GdW_{10}, two anionic moieties coordinate the central Gd^{3+} [see Fig. 1(a)]. Each moiety is twisted by an angle $\alpha = 44.2°$ with respect to the other, leading to a distorted square antiprism coordination (ideal D_{4d} symmetry). Under these

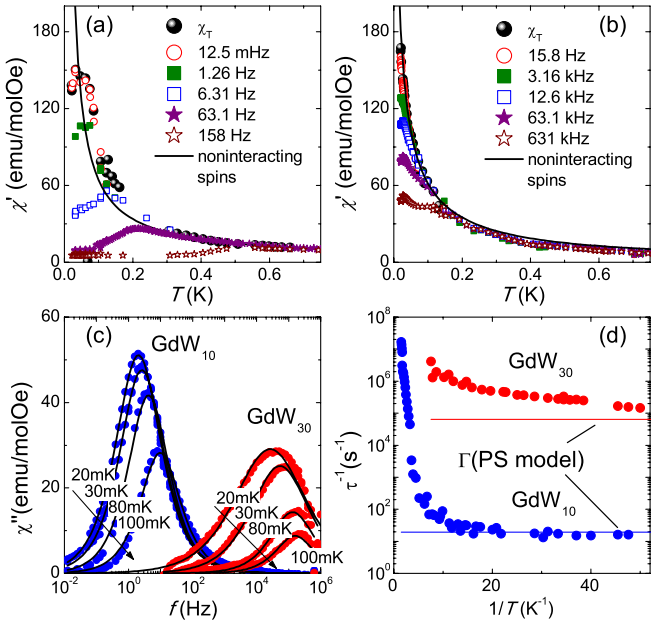

FIG. 2 (color online). Top: real component of the ac magnetic susceptibility (χ') measured at different frequencies on GdW_{10} (a) and GdW_{30} (b). The equilibrium susceptibility χ_T is obtained as the low frequency limit of χ'. Solid lines show χ_T calculated for noninteracting spins. Bottom: (c) imaginary part of the ac magnetic susceptibility measured at different temperatures on GdW_{10} and GdW_{30} (scatter) fitted to Cole-Cole laws (solid lines); (d) relaxation rates of GdW_{10} and GdW_{30} obtained from the Cole-Cole fits. Horizontal lines show the spin tunneling rates Γ that follow from Eq. (2).

circumstances, $\mathcal{H}$ includes an off-diagonal (i.e., noncommuting with S_z) term $B_4^4 \hat{O}_4^4$.

In the case of GdW_{30}, the first coordination shell of Gd^{3+} has a close to C_{5v} symmetry [see Fig. 1(c)], which allows the term $B_6^5 \hat{O}_6^5$. However, this term alone cannot account for the EPR data collected at varying temperatures and frequencies. Reasonably good fits are achieved introducing a second-order off-diagonal term $B_2^2 \hat{O}_2^2$. It is worth

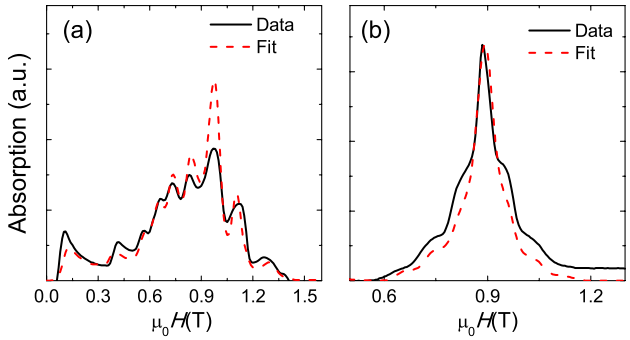

FIG. 3 (color online). Powder EPR absorption spectra of GdW_{10} (a) and GdW_{30} (b) at $T = 10$ K and $f = 25$ GHz. Black solid lines, experimental data; red dotted lines, fits based on Eq. (1).

recalling here that the magnetic anisotropy of Gd^{3+} arises via the quantum mixture of the ground state with excited multiplets, having a nonzero orbital moment L. These excited states are more sensitive than the ground state to interactions with ions located beyond the first coordination sphere. The departure of the whole GdW_{30} molecule from a pure C_{5v} symmetry must affect the wave functions of such excited states and be, therefore, a likely origin for the $B_2^2\hat{O}_2^2$ term.

The fits give $B_2^0/k_B = -0.059$ K and $B_4^4/k_B = 4 \times 10^{-4}$ K for GdW_{10}, and $B_2^0/k_B = 0.019$ K and $B_2^2/k_B = 0.019$ K for GdW_{30}. The inclusion of higher order terms does not improve the quality of the fits. Strong qualitative and quantitative differences exist between these two spin Hamiltonians. The former corresponds to an easy-axis magnetic anisotropy along the z axis [Fig. 1(a)]. The latter suggests that Gd_{30} possesses an easy-plane anisotropy with a preferred magnetization along y [Fig. 1(c)], x and z being the medium and hard magnetic axes, respectively. These crystal-field parameters account also for the specific heat data (not presented here).

The spin-lattice relaxation rates τ^{-1} can be determined, at each temperature, by fitting the frequency-dependent susceptibility data with a Cole-Cole law [26], as shown in Fig. 2(c). Values obtained by this method are shown in Fig. 2(d) as a function of temperature. Above $T \sim 200$ mK, the relaxation rate of GdW_{10} follows a thermally activated behavior $\tau^{-1} = \Gamma_0 \exp(-U/k_B T)$, with an activation energy $U/k_B = 2.2(2)$ K and a prefactor $\Gamma_0 = 3 \times 10^9$ s^{-1}. The activation energy agrees with the classical anisotropy energy barrier $U_{cl}/k_B = 2.15$ K derived from the spin Hamiltonian (1). Below that temperature τ^{-1} becomes nearly independent of temperature. This fact suggests that, in this temperature region, spin-lattice relaxation proceeds via pure quantum tunneling between the ground states, as it has been observed also for ErW_{10} [17]. In the same temperature region, τ^{-1} of GdW_{30} has not reached the pure quantum regime yet (it depends weakly on temperature) but nevertheless shows a strong deviation from the expected thermally activated behavior. Furthermore, it is 4 orders of magnitude faster than τ^{-1} of GdW_{10}. These results evidence that the coordination sphere strongly affects the classical and quantum spin dynamics of Gd^{3+} ions.

It might seem paradoxical, at first, that Gd^{3+} spins exhibit fast tunneling rates, as tunneling is strictly forbidden for a Kramer's ion at zero field. However, even if no external field is applied, each spin feels the dipolar magnetic field created by all other spins in the lattice. Below 0.3 K, χ_T of GdW_{10} [see Fig. 2(a)] deviates from the predictions for single spins, reaching a maximum at approximately $T_c \simeq 36$ mK, which signals the onset of long-range magnetic order. The characteristic width σ_{dip} of the dipolar field distribution can then be estimated using the relation $2g\mu_B S\sigma_{dip} \sim k_B T_c$, which gives $\sigma_{dip} \simeq 38$ Oe. Spin-spin interactions are weaker for GdW_{30}, on account of the larger intermolecular separations in this material (of order 2 nm vs 1 nm in GdW_{10}), and the dipolar ordering is accordingly not observed. As a first approximation, T_c can be estimated from that of GdW_{10}. As the dipolar interaction energy decreases with $1/r^3$, we expect $T_c \approx 4.5$ mK and $\sigma_{dip} \approx 4.8$ Oe. Transverse dipolar fields $H_{dip,\perp}$, i.e., perpendicular to the magnetization easy axis, give rise to a finite quantum tunnel splitting Δ of the initially degenerate doublets. Inserting in Eq. (1) a magnetic field of magnitude $H_{dip,\perp} = \sigma_{dip}$ oriented along the bisect of the hard and medium anisotropy axes gives $\Delta/k_B = 3.65 \times 10^{-6}$ K and $\Delta/k_B = 7.4 \times 10^{-5}$ K for the ground level doublets of GdW_{10} and GdW_{30}, respectively.

We can also estimate τ^{-1} in the quantum regime. At any given time, only those spins subject to a local dipolar bias $\xi_{dip} \lesssim \Delta$ can flip via tunneling. The reversal of these spins changes the spatial distribution of dipolar bias fields, thereby giving new spins the opportunity to flip. The average tunneling rate for the spin ensemble is then [27]

$$\Gamma = \frac{\Delta^2}{\hbar\sqrt{2\pi}\xi_{dip}(\sigma_{dip})}, \tag{2}$$

where $\xi_{dip}(\sigma_{dip}) = 2g\mu_B S\sigma_{dip}$. Inserting in Eq. (2) the values of Δ and $\xi_{dip}(\sigma_{dip})$ obtained for GdW_{10} gives $\Gamma = 19$ s^{-1} in agreement with the spin-lattice relaxation $\tau^{-1} \simeq 15$ s^{-1} measured below 200 mK [see Fig. 2(d)]. The same method gives $\Gamma = 6.4 \times 10^4$ s^{-1} for GdW_{30}, in fair agreement with $\tau^{-1} \simeq 10^5$ s^{-1} measured at $T = 20$ mK.

We are in a position to discuss the suitability of these molecules as spin qubits. The energy gap ΔE between the two qubit levels must fulfill the condition $2 \lesssim \Delta E/h \lesssim 20$ GHz to comply with the requirements of rf technologies and, in particular, with the resonance frequencies of superconducting microcavities that are currently seen as one of the most promising technologies for the development of scalable quantum computation architectures [28,29]. Also, its coupling to a rf magnetic field $\mathbf{h}_{rf}$ must be strong enough to ensure that the Rabi frequency $\Omega_R \equiv 2g\mu_B|\langle 1|\mathbf{h}_{rf}\mathbf{S}|0\rangle|/h$ of coherent rotations between qubit states $|0\rangle$ and $|1\rangle$ be much larger than the decoherence rates.

For the qubit definition, we might associate $|0\rangle$ and $|1\rangle$ with spin states belonging to the ground and first excited doublets (see Fig. 1). The qubit energy gap is then defined by the zero-field energy splitting, which amounts to $\Delta E/h = 22$ GHz and $\Delta E/h = 6.3$ GHz, for GdW_{10} and GdW_{30}, respectively. With the above technical considerations in mind, GdW_{30} appears as a close-to-ideal candidate because of its weak magnetic anisotropy, resulting from its peculiar molecular structure. The twofold degeneracies can be broken via the application of a weak magnetic field along the y easy axis. For instance, $\mu_0 H_y = 10$ mT splits the ground level doublet by 2 GHz, which would enable a ground state initialization of about 99.99% at $T = 10$ mK.

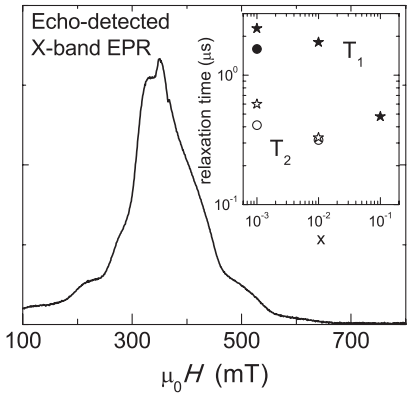

FIG. 4. Main panel: echo-detected X-band EPR spectrum measured on a powdered sample of $Gd_{0.001}Y_{0.999}W_{30}$ at $T = 6$ K using a two-pulses Hahn echo sequence with a $\pi/2$ pulse length of 16 ns and an interpulse delay of 180 ns. Inset: relaxation times T_1 (solid symbols) and T_2 (open symbols) of three $Gd_xY_{1-x}W_{30}$ samples measured at $T = 6$ K and for two magnetic fields, $\mu_0 H = 100$ mT (dots) and $\mu_0 H = 347$ mT (stars).

ΔE can be continuously tuned from 6.7 GHz, at $\mu_0 H_y = 10$ mT, up to 20 GHz, at $\mu_0 H_y = 465$ mT, becoming resonant with X-band photons for $\mu_0 H_y \simeq 100$ mT. These qubits can therefore be manipulated with the electromagnetic radiation produced by any conventional EPR setup [4–6,20], a flux qubit [30], or a superconducting microcavity [29]. The fact that large magnetic fields are not required to tune ΔE might enable the integration of these lanthanide-based spin qubits into superconducting quantum circuits. For the frequency of coherent oscillations we find, irrespective of H_y, $\Omega_R/h_{rf} \simeq 60$ MHz/mT when h_{rf} is applied along the z axis, and $\Omega_R/h_{rf} \simeq 90$ MHz/mT when h_{rf} is applied along the x axis. It might be noted here that if, by contrast, qubit states were associated with the ground state doublet $\langle S_y \rangle \approx \pm 3.45$, the tuning of ΔE would lead to a strong suppression of Ω_R unless relatively large (of the order of 1 T) and extremely well oriented transverse magnetic fields (i.e., along either z or x) were applied.

The values of Ω_R need to be compared with the dominant decoherence rates. Pulsed X-band EPR experiments ($\omega/2\pi = 9.8$ GHz) were performed on pure and magnetically diluted samples $Gd_xY_{1-x}W_{30}$. Echo signals were observed for $x \leq 0.1$. As an illustrative example, we show in Fig. 4 the echo-detected EPR powder spectrum of $Gd_{0.001}Y_{0.999}W_{30}$ measured at $T = 6$ K. The qubit transition defined above corresponds to the lowest edge of the absorption band between 100 mT and 700 mT. The echo relaxation measured at $\mu_0 H = 100$ mT gives $T_2 \simeq 410$ ns and $T_1 \simeq 1.6$ μs. Both relaxation times are observed to increase with decreasing concentration (see the inset of Fig. 4), suggesting that dipole-dipole interactions, albeit very weak, constitute an important source of decoherence. The qubit figure of merit [20] is then $Q_M \equiv 2\Omega_R T_2 \gtrsim 50$ for $h_{rf} = 1$ mT.

Summarizing, we have shown that GdW_{10} and GdW_{30} molecules behave as single molecule magnets at low temperatures. The magnetic anisotropy as well as the rates of magnetic relaxation and quantum tunneling are determined by the local coordination of the Gd^{3+} ion. These results show therefore that the molecular structure provides a parameter to control the underlying physics. The ability to tune the magnetic properties by chemical design offers fascinating perspectives for studies of quantum phenomena like tunneling, relaxation, and coherence, and for the optimization of lanthanide spin qubits.

The present work has been partly funded trough the Spanish MINECO (Grants No. MAT2009-13977-C03, MAT2007-61584, MAT2011-23861, and the CONSOLIDER project on Molecular Nanoscience), the EU (Project ELFOS and ERC Advanced Grant SPINMOL), the Generalidad Valenciana (Prometeo Programme), and the Gobierno de Aragón (Project MOLCHIP).

*eugenio.coronado@uv.es
†fluis@unizar.es

[1] R. Sessoli and D. Gatteschi, Angew. Chem. **42**, 268 (2003).
[2] J. R. Friedman, M. P. Sarachik, J. Tejada, and R. Ziolo, Phys. Rev. Lett. **76**, 3830 (1996); J. M. Hernández, X. X. Zhang, F. Luis, J. Bartolomé, J. Tejada, and R. Ziolo, Europhys. Lett. **35**, 301 (1996); L. Thomas, F. Lionti, R. Ballou, D. Gatteschi, R. Sessoli, and B. Barbara, Nature (London) **383**, 145 (1996).
[3] W. Wernsdorfer and R. Sessoli, Science **284**, 133 (1999).
[4] A. Ardavan, O. Rival, J. J. L. Morton, S. J. Blundell, A. M. Tyryshkin, G. A. Timco, and R. E. P. Winpenny, Phys. Rev. Lett. **98**, 057201 (2007).
[5] S. Bertaina, S. Gambarelli, T. Mitra, B. Tsukerblat, A. Muller, and B. Barbara, Nature (London) **453**, 203 (2008).
[6] C. Schlegel, J. van Slageren, M. Manoli, E. K. Brechin, and M. Dressel, Phys. Rev. Lett. **101**, 147203 (2008).
[7] E. Burzurí, F. Luis, B. Barbara, R. Ballou, E. Ressouche, O. Montero, J. Campo, and S. Maegawa, Phys. Rev. Lett. **107**, 097203 (2011).
[8] M. N. Leuenberger and D. Loss, Nature (London) **410**, 789 (2001).
[9] J. Tejada, E. M. Chudnovsky, E. del Barco, J. M. Hernández, and T. P. Spiller, Nanotechnology **12**, 181 (2001).
[10] F. Troiani, A. Ghirri, M. Affronte, S. Carretta, P. Santini, G. Amoretti, S. Piligkos, G. Timco, and R. E. P. Winpenny, Phys. Rev. Lett. **94**, 207208 (2005).
[11] M. Affronte, J. Mater. Chem. **19**, 1731 (2009); A. Ardavan and S. J. Blundell, *ibid.***19**, 1754 (2009); P. C. E. Stamp and A. Gaita-Ariño, *ibid.***19**, 1718 (2009).
[12] F. Luis, A. Repollés, M. J. Martínez-Pérez, D. Aguilà, O. Roubeau, D. Zueco, P. J. Alonso, M. Evangelisti, A. Camón, J. Sesé, L. A. Barrios, and G. Aromí, Phys. Rev. Lett. **107**, 117203 (2011).
[13] P. Santini, S. Carretta, F. Troiani, and G. Amoretti, Phys. Rev. Lett. **107**, 230502 (2011).

[14] N. Ishikawa, M. Sugita, and W. Wernsdorfer, Angew. Chem., Int. Ed. Engl. **44**, 2931 (2005).
[15] M. A. AlDamen, J. M. Clemente-Juan, E. Coronado, C. Martí-Gastaldo, and A. Gaita-Ariño, J. Am. Chem. Soc. **130**, 8874 (2008).
[16] M. A. AlDamen, S. Cardona-Serra, J. M. Clemente-Juan, E. Coronado, C. Martí-Gastaldo, F. Luis, and O. Montero, Inorg. Chem. **48**, 3467 (2009).
[17] F. Luis, M. J. Martínez-Pérez, O. Montero, E. Coronado, S. Cardona-Serra, C. Martí-Gastaldo, J. M. Clemente-Juan, J. Sesé, D. Drung, and T. Schurig, Phys. Rev. B **82**, 060403 (2010).
[18] N. V. Prokofév and P. C. E. Stamp, Rep. Prog. Phys. **63**, 669 (2000).
[19] B. Bleaney, H. E. D. Scovil, and R. S. Trenam, Proc. R. Soc. A **223**, 15 (1954).
[20] S. Bertaina, S. Gambarelli, A. Tkachuk, I. N. Kurkin, B. Malkin, A. Stepanov, and B. Barbara, Nature Nanotech. **2**, 39 (2007).
[21] M. J. Martínez-Pérez, J. Sesé, F. Luis, D. Drung, and T. Schurig, Rev. Sci. Instrum. **81**, 016108 (2010).
[22] M. J. Martínez-Pérez, J. Sesé, F. Luis, R. Córdoba, D. Drung, T. Schurig, E. Bellido, R. de Miguel, C. Gómez-Moreno, A. Lostao, and D. Ruiz-Molina, IEEE Trans. Appl. Supercond. **21**, 345 (2011).
[23] C. Schlegel, M. Dressel, and J. van Slageren, Rev. Sci. Instrum. **81**, 093901 (2010).
[24] S. Stoll and A. Schweiger, J. Magn. Reson. **178**, 42 (2006).
[25] K. W. H. Stevens, Proc. Phys. Soc. London Sect. A **65**, 209 (1952).
[26] K. S. Cole and R. H. Cole, J. Chem. Phys. **9**, 341 (1941).
[27] N. V. Prokof'ev and P. C. E. Stamp, Phys. Rev. Lett. **80**, 5794 (1998).
[28] R. J. Schoelkopf and S. M. Girvin, Nature (London) **451**, 664 (2008).
[29] D. I. Schuster *et al.*, Phys. Rev. Lett. **105**, 140501 (2010); Y. Kubo *et al.*, *ibid.* **105**, 140502 (2010); H. Wu *et al.*, *ibid.* **105**, 140503 (2010).
[30] X. Zhu, S. Saito, A. Kemp, K. Kakuyanagi, S. Karimoto, H. Nakano, W. J. Munro, Y. Tokura, M. S. Everitt, K. Nemoto, M. Kasu, N. Mizuochi, and K. Semba, Nature (London) **478**, 221 (2011).